Phosphorus-Stabilized Geminal Dianions

Thibault Cantat, Louis Ricard, Pascal Le Floch, and Nicolas Mézailles*

Département de Chimie, Ecole Polytechnique Laboratoire "Hétéroéléments et Coordination", UMR CNRS 7653 (DCPH), 91128 Palaiseau Cédex, France

Received May 23, 2006

After a presentation of the structures of the known dilithiomethane derivatives, full details on the synthesis and crystal structures of a bis(thiophosphinoyl)-stabilized geminal dianion (**2**) as well as the first synthesis of an analogous bis(phosphonate) derivative (**6**) are exposed. Two X-ray crystal structures were obtained for **2**. They both exhibit a dimeric arrangement with different solvation states. Variable-temperature NMR experiments (^{31}P and ^{7}Li) show that in solution either several species (in a 1:1 equilibrium) or a single species (one aggregate with different Li/P environments) forms. DFT calculations have been performed on these dianions, and a precise electronic structure is presented on the basis of NBO analysis. The nucleophilic reactivity of these dianions toward CS_2 readily provides new 1,1-ethylenedithiolate type compounds (**7** and **8**).

Introduction

In organic chemistry, the development of strategies which minimize the number of steps for the syntheses of increasingly complex molecular structures is crucial. With this aim, chemical transformations that are performed successively in one pot appear both efficient and elegant. The use of geminated organodimetallics, which usually possess different successive reactivities, has attracted increasing interest and met with success. This area has been reviewed by Marek and Normant in 1996.[1] More recently, Matsubara and co-workers developed the use of bis(iodozincio)methane in sequential transition-metal-catalyzed cross-coupling reactions.[2] Wittig,[3] West,[4] and Ziegler[5] developed syntheses of dilithiomethane more than 50 years ago, but its use in organic synthesis was hampered by both its high reactivity and its instability. In terms of structural characterization, initial computational studies by Schleyer and co-workers predicted planar and tetrahedral structures of dilithiomethane to be close in energy for monomeric species ($\Delta E = 8$ kcal mol^{-1} in favor of the tetrahedral structure).[6,7] Later, dimeric and trimeric species were considered,[8] consistent with the experimental observation of the low solubility of the compound in inert solvents. Solid-state NMR studies followed by X-ray powder diffraction data led to a proposed X-ray structure for CD_2Li_2,[9,10] but the final structure has not been determined yet. Several derivatives are now known, such as 1,1-dilithio-2,2,3,3-tetramethylcyclopropane (1,1-dilithiopropane is predicted to prefer the planar geometry at carbon)[11] and $tBuCHLi_2$ and $TMSCHLi_2$,[12] but their structures are still unknown. In a recent report, Linti and co-workers have reported the first crystal structure of an α,α-dilithiated hydrocarbon, 9,9-dilithiofluorene (**I**), obtained by dismutation of lithiofluorene in THF/benzene medium (Scheme 1).[13]

Scheme 1

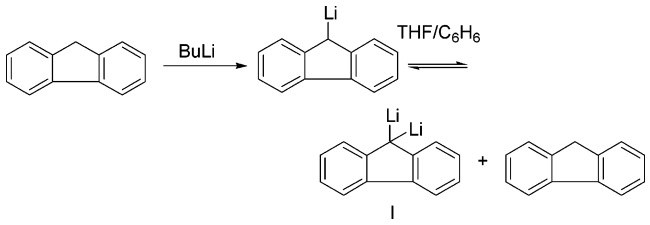

I

Scheme 2

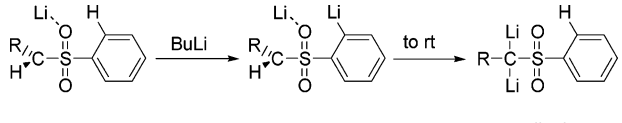

α,o-dianion α,α-dianion

II

In terms of synthetic potential, heteroatom-substituted dilithio derivatives could be more interesting. Indeed, these substituents may be further modified, but this area of research has still to be pursued. The sulfone derivatives **II** have been known for some time,[14] and the related chiral sulfoximine species **III** has been developed recently (Scheme 2 and Chart 1).[15] Interestingly, with the sulfone derivatives, Gais et al. showed in 1988 that the reaction of BuLi with lithiosulfone derivatives could lead to other products: the α,o-"dianion", which subsequently forms the desired α,α-dilithiated species **II** upon raising the temperature, for which they also obtained a crystal structure.[16]

* To whom correspondence should be addressed. Tel: +33 1 69 33 40 79. Fax: +33 1 69 33 39 90. E-mail: mezaille@poly.polytechnique.fr.

(1) Marek, I.; Normant, J. F. *Chem. Rev.* **1996**, *96*, 3241.
(2) Yoshino, H.; Toda, N.; Kobata, M.; Ukai, K.; Oshima, K.; Utimoto, K.; Matsubara, S. *Chem. Eur. J.* **2006**, *12*, 721.
(3) Wittig, G.; Harborth, G. *Chem. Ber.* **1944**, *77*, 306.
(4) West, R.; Rochow, E. G. *J. Org. Chem.* **1953**, *18*, 1739.
(5) Ziegler, K.; Nagel, K.; Patheiger, M. *Z. Anorg. Allg. Chem.* **1955**, *282*, 345.
(6) Collins, J. B.; Dill, J. D.; Jemmis, E. D.; Apeloig, Y.; Schleyer, P. v. R.; Seeger, R.; Pople, J. A. *J. Am. Chem. Soc.* **1976**, *98*, 5419.
(7) Laidig, W. D.; Schaefer, H. F. *J. Am. Chem. Soc.* **1978**, *100*, 5972.
(8) Jemmis, E. D.; Schleyer, P. v. R.; Pople, J. A. *J. Organomet. Chem.* **1978**, *154*, 327.
(9) Stucky, G. D.; Eddy, M. M.; Harrison, W. H.; Lagow, R.; Kawa, H.; Cox, D. E. *J. Am. Chem. Soc.* **1990**, *112*, 2425.
(10) Gurak, J. A.; Chinn, J. W.; Lagow, R. J.; Steinfink, H.; Yannoni, C. S. *Inorg. Chem.* **1984**, *23*, 3717.
(11) Kawa, H.; Manley, B. C.; Lagow, R. J. *J. Am. Chem. Soc.* **1985**, *107*, 5313.
(12) Kawa, H.; Manley, B. C.; Lagow, R. J. *Polyhedron* **1988**, *7*, 2023.
(13) Linti, G.; Rodig, A.; Pritzkow, H. *Angew. Chem., Int. Ed.* **2002**, *41*, 4503.
(14) Boche, G. *Angew. Chem., Int. Ed. Engl.* **1989**, *28*, 277.
(15) Muller, J. F. K.; Neuburger, M.; Spingler, B. *Angew. Chem., Int. Ed.* **1999**, *38*, 3549.

10.1021/om060450l CCC: $33.50
Publication on Web 09/13/2006

Chart 1

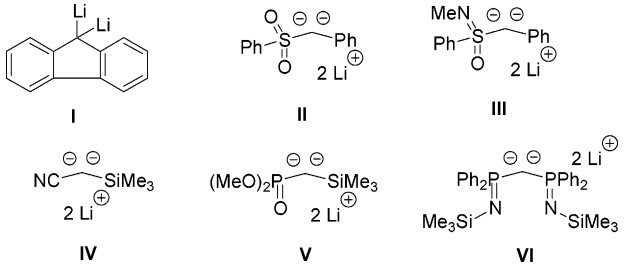

The α,o-"dianion" mimics the reactivity of the α,α-dilithiated species, as can also be found for quasi-dianion complexes. These examples stress the utmost importance of the precise knowledge of the structure of the dianionic dilithio derivatives. Boche et al. reported in 1989 the double deprotonation of the (trimethylsilyl)acetonitrile species **IV** and presented the X-ray structure: the dodecamer $(SiMe_3CLi_2CN)_{12}\cdot 6Et_2O\cdot C_6H_{14}$.[17] Müller and co-workers reported recently the first structures of the dilithiated phosphonate and chiral sulfoximine derivatives **V**[18] and **III**,[15] respectively. The structure of the latter species was obtained after reaction with an excess of BuLi in the presence of traces of water. This partial hydrolysis of the base resulted in the formation of Li_2O, which was found to be crucial for crystallization. Simultaneously, and independently, Cavell et al. and Stephan et al. reported the synthesis of the dianion of the bis(iminophosphorane) derivative **VI**.[19,20] The solid-state structure consists of an unsolvated dimer of the dianion, in which the nitrogen atom of the iminophosphorane moiety completes the lithium coordination sphere.

Although some of these dianionic species have been known for several decades, the studies on their coordination chemistry are very limited. Müller and co-workers have reacted both the sulfoximine derivative **III** and phosphonate derivative **V** with a stoichiometric amount of the titanium (IV) precursor $[ClTi(OiPr)_3]$.[21] Transmetalation was observed, and for the latter case, a crystal structure of the mixed lithium titanium phosphonate was obtained. The reactivity of the analogous lithium titanium sulfoximine with aldehyde was studied. Most of the reports regarding the coordination chemistry of geminal dianions have been concerned with the bis(iminophosphorane) derivative **VI**. Cavell et al. have used this compound to synthesize several alkylidene complexes: Sm(III), Zr, Ti, and Hf(IV), as well as a Pt(II) complex.[22−31] Leung and co-workers reported the Mo(0) complex from the bis(germavinylidene) precursor $[(Me_3SiN{=}PPh_2)_2C{=}Ge{\rightarrow}Ge{=}C(PPh_2{=}NSiMe_3)_2]$.[32] Dianion **VI** was also shown to act as a bridging ligand for Al and Cr centers.[33−35] This behavior had been observed earlier by Robinson et al. in their in situ double deprotonation/coordination sequence with $AlMe_3$ of neutral $CH_2(Ph_2P{=}E)_2$ (E = O, S).[36,37] Recently, we synthesized a bis(thiophosphinoyl)methanediide dianion (**2**) and developed its coordination chemistry with Pd(II), Ru(II), Sm(III), and Tm(III) metal centers.[38−41]

Scheme 3

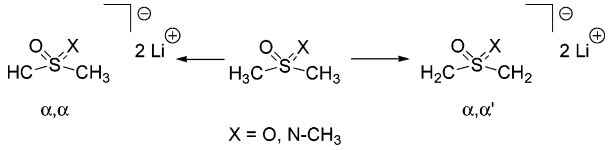

As mentioned above, the electronic structure of the parent monomeric dilithiomethane was investigated by theoretical calculations, but it was later shown that the species is not monomeric in inert solvents. Bors and Streitwieser performed a theoretical study of the dilithio derivatives of dimethyl sulfone and found the α,α derivative to be 9 kcal mol^{-1} higher in energy than the α,α′ derivative.[42] Müller and co-workers later reported an ab initio study on monomeric dilithiosulfoximine, in which they found that the geminal dianion (α,α) was only 2.7 kcal mol^{-1} higher in energy than the α,α′ dianion (Scheme 3).[43] Klobukowski et al. studied both the monomer and the dimer of the dianion **VI** by DFT and compared the optimized geometries to the experimental structure. However, the precise electronic nature of the α,α dianions was not discussed in these reports.[44]

It is our purpose here to present full details on the synthesis of a bis(thiophosphinoyl)methanediide dianion, as well as two different X-ray crystal structures for this species. We also report the first synthesis of a bis(phosphonate) geminal dianion. DFT calculations have been performed for the thiophosphinoyl derivative, first on the dimeric species in order to compare the results to the X-ray structure and then on the monomeric species to determine the effects of aggregation. The calculations performed on the monomeric bis(phosphonate) geminal dianion are also presented. A precise electronic structure of these

(16) Gais, H. J.; Vollhardt, J.; Gunther, H.; Moskau, D.; Lindner, H. J.; Braun, S. *J. Am. Chem. Soc.* **1988**, *110*, 978.
(17) Zarges, W.; Marsch, M.; Harms, K.; Boche, G. *Chem. Ber.* **1989**, *122*, 1307.
(18) Muller, J. F. K.; Neuburger, M.; Spingler, B. *Angew. Chem., Int. Ed.* **1999**, *38*, 92.
(19) Ong, C. M.; Stephan, D. W. *J. Am. Chem. Soc.* **1999**, *121*, 2939.
(20) Kasani, A.; Babu, R. P. K.; McDonald, R.; Cavell, R. G. *Angew. Chem., Int. Ed.* **1999**, *38*, 1483.
(21) Muller, J. F. K.; Kulicke, K. J.; Neuburger, M.; Spichty, M. *Angew. Chem., Int. Ed.* **2001**, *40*, 2890.
(22) Aparna, K.; Ferguson, M.; Cavell, R. G. *J. Am. Chem. Soc.* **2000**, *122*, 726.
(23) Aparna, K.; Babu, R. P. K.; McDonald, R.; Cavell, R. G. *Angew. Chem., Int. Ed.* **2001**, *40*, 4400.
(24) Babu, R. P. K.; McDonald, R.; Decker, S. A.; Klobukowski, M.; Cavell, R. G. *Organometallics* **1999**, *18*, 4226.
(25) Babu, R. P. K.; McDonald, R.; Cavell, R. G. *Organometallics* **2000**, *19*, 3462.
(26) Babu, R. P. K.; McDonald, R.; Cavell, R. G. *Chem. Commun.* **2000**, 481.
(27) Cavell, R. G.; Babu, R. P. K.; Aparna, K. *J. Organomet. Chem.* **2001**, *617*, 158.
(28) Fang, M.; Jones, N. D.; Ferguson, M. J.; McDonald, R.; Cavell, R. G. *Angew. Chem., Int. Ed.* **2005**, *44*, 2005.
(29) Jones, N. D.; Lin, G. Y.; Gossage, R. A.; McDonald, R.; Cavell, R. G. *Organometallics* **2003**, *22*, 5378.
(30) Jones, N. D.; Cavell, R. G. *J. Organomet. Chem.* **2005**, *690*, 5485.
(31) Lin, G. Y.; Jones, N. D.; Gossage, R. A.; McDonald, R.; Cavell, R. G. *Angew. Chem., Int. Ed.* **2003**, *42*, 4054.
(32) Leung, W. P.; So, C. W.; Wang, J. Z.; Mak, T. C. W. *Chem. Commun.* **2003**, 248.
(33) Aparna, K.; McDonald, R.; Ferguson, M.; Cavell, R. G. *Organometallics* **1999**, *18*, 4241.
(34) Aparna, K.; McDonald, R.; Cavell, R. G. *J. Am. Chem. Soc.* **2000**, *122*, 9314.
(35) Kasani, A.; McDonald, R.; Cavell, R. G. *Chem. Commun.* **1999**, 1993.
(36) Robinson, G. H.; Lee, B. S.; Pennington, W. T.; Sangokoya, S. A. *J. Am. Chem. Soc.* **1988**, *110*, 6260.
(37) Robinson, G. H.; Self, M. F.; Pennington, W. T.; Sangokoya, S. A.; *Organometallics* **1988**, *7*, 2424.
(38) Cantat, T.; Demange, M.; Mézailles, N.; Ricard, L.; Jean, Y.; Le Floch, P. *Organometallics* **2005**, *24*, 4838.
(39) Cantat, T.; Jaroschik, F.; Nief, F.; Ricard, L.; Mézailles, N.; Le Floch, P. *Chem. Commun.* **2005**, 5178.
(40) Cantat, T.; Jaroschik, F.; Ricard, L.; Le Floch, P.; Nief, F.; Mézailles, N. *Organometallics* **2006**, *25*, 1329.
(41) Cantat, T.; Mézailles, N.; Ricard, L.; Jean, Y.; Le Floch, P. *Angew. Chem., Int. Ed.* **2004**, *43*, 6382.
(42) Bors, D. A.; Streitwieser, A. *J. Am. Chem. Soc.* **1986**, *108*, 1397.
(43) Muller, J. F. K.; Batra, R. *J. Organomet. Chem.* 1999, *584*, 27.
(44) Klobukowski, M.; Decker, S. A.; Lovallo, C. C.; Cavell, R. G. *J. Mol. Struct. (THEOCHEM)* **2001**, *536*, 189.

Scheme 4

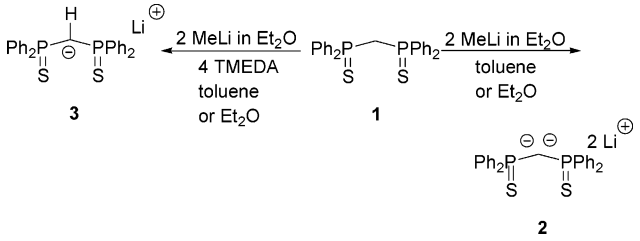

Scheme 5

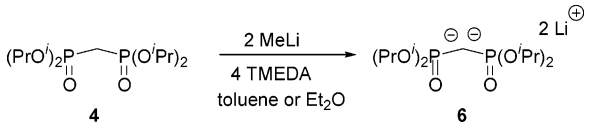

dianions is described on the basis of NBO calculations. Finally, the nucleophilic reactivity of these dianions toward CS_2, leading to new 1,1-ethylenedithiolate-type compounds, is reported.

Results and Discussion

Syntheses of the Dianions. The synthesis of the geminal dianion **2** is quite straightforward. It relies on the double deprotonation of the neutral compound **1** with stoichiometric amounts of MeLi (in Et_2O) in diethyl ether or toluene. The reaction is fast, taking 3 h in toluene and 20 min in diethyl ether (Scheme 4). The formation of **2** is easily followed by ^{31}P NMR spectroscopy, as it is soluble in the reaction medium. As has been reviewed recently by van Koten and co-workers, the state of aggregation of MeLi in solution can influence the kinetics of the reaction, and additives, able to break the aggregates, are often used to enhance its reactivity in a given solvent.[45] Here, however, the addition of 2 equiv of TMEDA per equivalent of MeLi in diethyl ether resulted in the fast precipitation of a white solid. This compound was subsequently shown to be the monoanionic derivative **3** (δ_P 38 ppm).

Evaporation of a solution of **2** in a toluene/diethyl ether mixture leads to partial degradation of the dianion to its monoanionic form (**3**). However, **2** could be isolated as a solid by evaporating the solvent from a solution of **2** in diethyl ether. This allowed full characterization by the usual NMR techniques. In the ^{31}P NMR spectrum a singlet, shielded upfield from the starting material by 12 ppm (δ 23 ppm), is observed. In the ^1H NMR spectrum, the characteristic triplet (due to the coupling with the two equivalent phosphorus centers) of the two methylenic protons of **1** is no longer observed. Despite extensive drying, the solvation of the compound by 1.5 equiv of diethyl ether was clearly evidenced in the proton spectrum. Unlike what was noted previously in the case of dianion **VI**, the signal of the quaternary P−C−P carbon atom was observed in the ^{13}C NMR spectrum. It is characterized by a triplet with a large $^1J_{C-P}$ coupling constant of 41 Hz at a high field (δ 30.3 ppm).

The dianion of the bis(phosphonate) derivative **4** was found to be more difficult to access (Scheme 5). The reaction with MeLi proved to be quite slow, being incomplete even after 10 days at room temperature. The addition of 2 equiv of TMEDA (per MeLi) proved very beneficial, leading to completion of the reaction after 3 days at room temperature. Following the reaction by ^{31}P NMR spectroscopy indicated a very fast formation of the monoanionic species **5**, whose signal slowly decreased over time, with the concomitant formation of a white precipitate. This indicated that the desired dianion **6** precipitated from the reaction medium as it formed. Dianion **6** is completely insoluble in solvents with which it does not react (Et_2O, dme = dimethoxyethane, toluene, benzene) and was therefore characterized by elemental analyses and further reactivity tests (vide infra).

Scheme 6

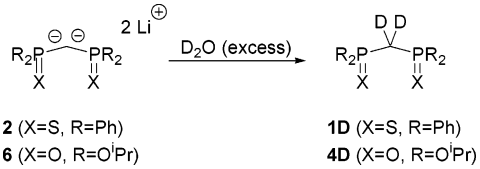

The yields of the isolated dianions were excellent, being over 94%, without needing further purification. As expected, both species are extremely reactive, abstracting quantitatively a proton from THF or pyridine, to re-form the monoanions **3** and **5**, respectively. Further proof of the formation of **6** (as of **2**), is given by the quantitative reaction with D_2O, which leads to the corresponding deuterated starting material **4D** (and **1D**, respectively) (Scheme 6). Indeed, in the ^{31}P NMR spectrum, signals at 17.9 ppm for **4D** and 35.1 ppm for **1D** were observed, whereas in the ^1H NMR spectrum, the absence of the CH_2 moiety was noted as expected. Moreover, neither the peaks for TMEDA nor the solvent peaks were observed upon trapping a suspension of **6** in C_6D_6 by D_2O, which indicates that **6** precipitates as a nonsolvated, most likely polymeric species.[46] Furthermore, drying does not cause any degradation of **6**.

X-ray-quality crystals were obtained by the slow diffusion of hexane into a solution of **2** in a mixture of toluene/Et_2O (form **2A**, Figure 1). Information concerning the data collection and refinement are given in the Supporting Information. In form **2A**, dianion **2** is crystallized as a dimer in which the two carbon atoms are bridged by two lithium atoms while the two other lithium atoms bridge two sulfur centers. This structure differs remarkably from that obtained for the bis(iminophosphorane)-methanediide dimer **VI**, in which a pseudo-octahedral Li_4C_2 core

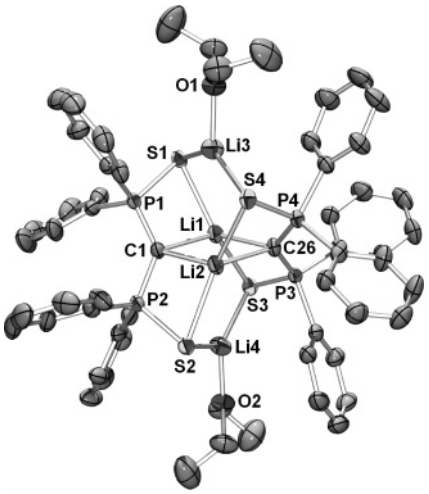

Figure 1. View of one molecule of **2A**·Et_2O (thermal ellipsoids set at 50% probability). The hydrogen atoms are omitted for clarity. Selected bond lengths (Å) and angles (deg): C1−Li1 = 2.195(5), C1−Li2 = 2.159(5), C26−Li1 = 2.196(5), C26−Li2 = 2.173(5), C1−P1 = 1.672(3), C1−P2 = 1.678(3), C26−P3 = 1.678(3), C26−P4 = 1.676(3), P1−S1 = 2.037(1), P2−S2 = 2.040(1), P3−S3 = 2.041(1), P4−S4 = 2.039(1), S1−Li1 = 2.477(5), S1−Li3 = 2.454(5), S2−Li2 = 2.480(4), S2−Li4 = 2.454(5), S3−Li1 = 2.450(5), S3−Li4 = 2.461(5), S4−Li2 = 2.517(4), S4−Li3 = 2.426(5); P1−C1−P2 = 131.6(2), P3−C26−P4 = 131.3(2).

(45) Gossage, R. A.; Jastrzebski, J.; van Koten, G. *Angew. Chem., Int. Ed.* **2005**, *44*, 1448.

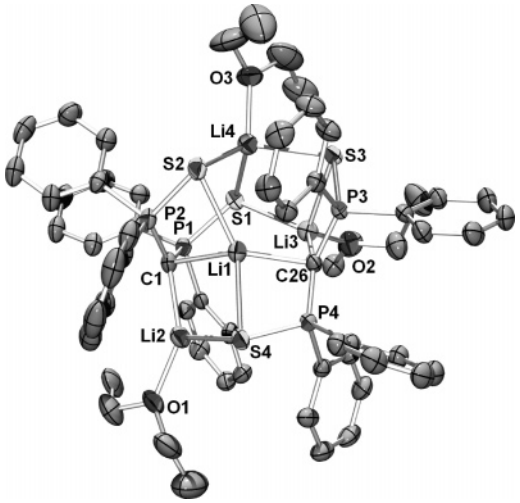

Figure 2. View of one molecule of **2B**·3Et_2O (thermal ellipsoids set at 50% probability). The hydrogen atoms are omitted for clarity. Selected bond lengths (Å) and angles (deg): C1−Li1 = 2.343(4), C1−Li2 = 2.120(4), C26−Li1 = 2.181(4), C26−Li3 = 2.200(4), C1−P1 = 1.681(2), C1−P2 = 1.693(2), C26−P3 = 1.683(2), C26−P4 = 1.685(2), P1−S1 = 2.048(2), P2−S2 = 2.036(1), P3−S3 = 2.032(1), P4−S4 = 2.038(1), S2−Li1 = 2.508(4), S4−Li1 = 2.560(4), S4−Li2 = 2.471(4), S1−Li3 = 2.550(4), S3−Li3 = 2.494(4), S1−Li4 = 2.441(4), S2−Li4 = 2.451(4), S3−Li4 = 2.505(4); P1−C1−P2 = 120.6(1), P3−C26−P4 = 130.6(1).

cluster was involved.[19,20] As could be envisioned, the double deprotonation leads to dramatic modifications in the bond lengths and angles of the bis(thiophosphinoyl)methylene backbone. Indeed, the P−C bond distances are shortened by 0.151 Å in **2A** (1.675 Å compared to 1.827 Å in **1**[47]). This bond distance is as short as those found in carbodiphosphoranes (R_3-$PCPR_3$, 1.64 Å[48−52]) and in **VI** (1.69 Å). On the other hand, the P−S bond distance is lengthened to 2.039 Å in **2A** (1.945 Å in 1) and the internal P−C−P bond angle is widened to 131.4° in **2A** (from 118.4° in **1**). No interaction between the individual lithium atoms (2.510 Å) or between the carbanion centers (3.567 Å) is found.

Two different coordination sites are found for the lithium centers in **2A**. The first site is stabilized by two carbon and two sulfur centers. In the second site, 1 equiv of Et_2O completes the coordination sphere of the lithium cation bound to the sulfur atoms. However, the ^{1}H NMR spectrum recorded for **2** (synthesized in Et_2O) indicates the presence of 1.5 equiv of Et_2O per dianion instead of the 1 equiv observed in the crystal structure (Figure 1). It seems therefore that the dianion retains less Et_2O when it is crystallized from a toluene/Et_2O mixture than when a pure Et_2O solution of **2** is evaporated to dryness. This prompted us to crystallize **2** from pure Et_2O by slow evaporation. A new X-ray structure was obtained (form **2B**, Figure 2 and the Supporting Information).

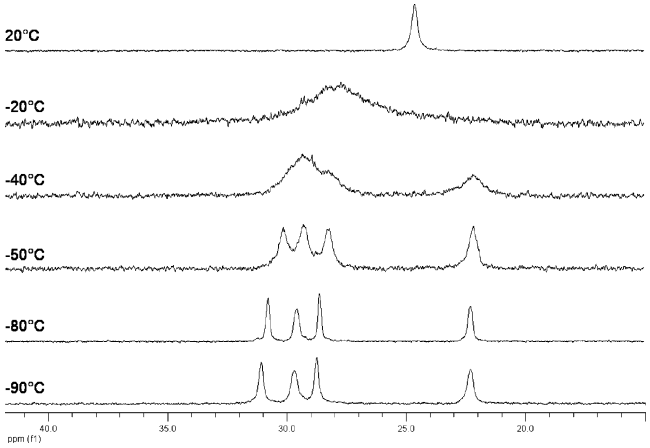

Figure 3. ^{31}P NMR spectra at different temperatures for a solution of **2** in a toluene/Et_2O (5:1) mixture at a concentration of 0.13 mol L^{-1} (relative intensities: 1.0:1.0:1.0:1.0).

Under these conditions, dianion **2** also crystallizes as a dimer (form **2B**), with a unit cell containing two dimers which possess very similar features. In each dimer, the two monomeric units present similar bond distances which are close to those measured for the form **2A**. However, they strongly differ from each other by the orientation of the P−S bonds relative to the P−C−P planes; indeed, the dihedral angles S−P−C−P vary from 60.8 to 175.3°. This leads to the presence of four inequivalent phosphorus centers in the dimer. Four different coordination sites are also found for the lithium cations. Li1 is coordinated to two carbon atoms (C1 and C26) and two sulfur atoms (S2 and S4); Li2 is coordinated to C1, S4, and one molecule of Et_2O. Li3 lies in a tetrahedral environment (C26, S1, S3, and one molecule of Et_2O). Finally, Li4 is stabilized by three sulfur atoms (S1, S2, S3) and one molecule of Et_2O. Overall, this results in the incorporation of 1.5 equiv of Et_2O per dianion in **2B**, consistent with the ^{1}H NMR spectrum of the dianion obtained after extensive drying of the ethereal solution. In the solid state, **2** therefore forms two different dimers, **2A** and **2B**, whose exact structure and stoichiometry depend markedly on the solvent used during synthesis.

To verify if aggregates of **2** also form in solution, the ^{7}Li NMR spectrum of compound **2** (toluene/Et_2O (5:1) mixture at a concentration of 0.13 mol L^{-1}) was recorded first at room temperature. A single resonance was observed, which shows that either the dimeric structure is broken or a fast exchange process (on the NMR time scale) between the two types of lithium centers occurs. This prompted us to carry out a variable-temperature experiment. The modification of the signal with the change in temperature was thus followed by both ^{31}P NMR and ^{7}Li NMR spectroscopy (Figures 3 and 4).

Starting from room temperature (20 °C) and lowering down to −20 °C leads to a significant shift in the ^{31}P NMR spectrum ($\Delta\delta$ = 3.1 ppm, δ(rt) 24.6 ppm) together with a broadening of the peak ($\nu_{1/2}$ = 35.1 Hz at 20 °C vs $\nu_{1/2}$ = 332 Hz at −20 °C). A similar broadening is also noted in the ^{7}Li NMR spectrum ($\nu_{1/2}$ = 9.3 Hz at 20 °C vs $\nu_{1/2}$ = 40.3 Hz at −20 °C), without a shift, however. Upon stepwise cooling to −90 °C several decoalescence processes are observed in the ^{31}P NMR and ^{7}Li NMR spectra. At low temperature (below −50 °C) four different ^{31}P signals were observed (^{31}P at −90 °C, δ 22.3, 28.6, 29.5, 30.8 ppm), together with at least four different ^{7}Li signals (^{7}Li at −90 °C, δ 0.15, 0.53, 0.64, 1.70 ppm). Careful integration of the ^{31}P spectrum indicated that the signals are in a 1.0:1.0:1.0:1.0 ratio. This suggests the formation of either several species which are in a 1:1 equilibrium or a single species (one

(46) Note that a polymeric form has been observed in the solid state for dianion **V**.

(47) Carmalt, C. J.; Cowley, A. H.; Decken, A.; Lawson, Y. G.; Norman, N. C. *Acta Crystallogr., Sect. C: Cryst. Struct. Commun.* **1996**, *52*, 931.
(48) Hardy, G. E.; Kaska, W. C.; Chandra, B. P.; Zink, J. I. *J. Am. Chem. Soc.* **1981**, *103*, 1074.
(49) Petz, W.; Kutschera, C.; Heitbaum, M.; Frenking, G.; Tonner, R.; Neumuller, B. *Inorg. Chem.* **2005**, *44*, 1263.
(50) Schmidbaur, H.; Costa, T.; Milewskimahrla, B.; Schubert, U. *Angew. Chem., Int. Ed. Engl.* **1980**, *19*, 555.
(51) Schubert, U.; Kappenstein, C.; Milewskimahrla, B.; Schmidbaur, H. *Chem. Ber./Recl.* **1981**, *114*, 3070.
(52) Vincent, A. T.; Wheatley, P. J. *J. Chem. Soc., Dalton Trans.* **1972**, 617.

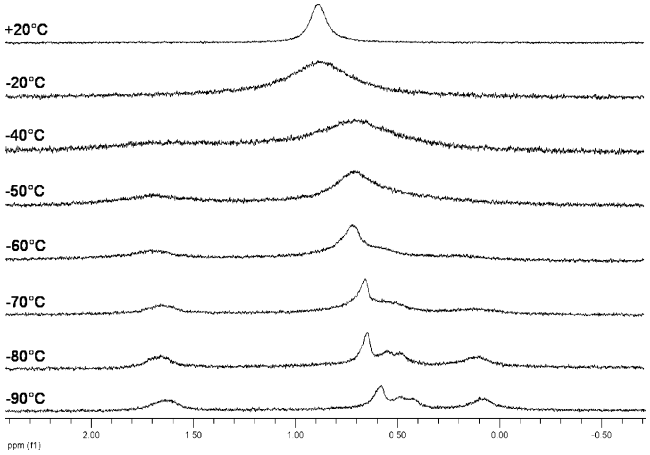

Figure 4. ^{7}Li NMR spectra at different temperatures for a solution of **2** in a toluene/Et_2O (5:1) mixture at a concentration of 0.13 mol L^{-1}.

aggregate with different Li/P environments). Moreover, these data show that the symmetrical dimeric form **2A** found in the solid state is not preserved in solution, even at low temperature. However, we propose that the structure of the aggregate found at low temperature is close to that observed in the solid-state form **2B**, in which four different P and Li atoms are present.

DFT Calculations: Electronic Structures of the Dianions. To fully rationalize the variations in geometrical parameters between neutral and dianionic species and to propose a detailed electronic structure for these dianions, DFT calculations were performed (at the B3PW91[53,54]/6-31+G* level of theory). First, the neutral compound **E** and the dimeric dianions **A** and **B** were calculated in order to compare the optimized geometries to the solid-state structures. Then the nonsolvated monomeric dianion **C** was optimized to test whether significant modifications in the electronic distribution would be observed. The analogous neutral species (**F**) and monomeric dianion (**D**) of the bis(phosphonate) derivative were also optimized, in order to quantify the differences between the two classes of compounds studied here. These compounds were optimized first without symmetry constraints. Then, except for **B**, these model compounds were optimized under symmetry constraints: dimer **A** was optimized with a D_2 point group constraint, and the monomeric species were optimized with the C_2 point group constraint. No significant difference was noted with the unconstrained structures in terms of energy (<1 kcal mol^{-1}) and geometrical parameters. The optimized structures are presented in Chart 2. For the sake of simplicity, the discussion will concern the symmetry-constrained, optimized models.

The optimized geometry for dimer **A** is in excellent agreement with the X-ray structure (cf. Table 1). In particular, both the very short P−C bonds (1.687 Å) and the long P−S bonds (2.048 Å) are very well reproduced. The lack of Li···Li and C···C interactions is also noted (2.542 and 3.527 Å, respectively) and confirmed by Wiberg bond indexes calculated as 0.00. In the constrained D_2 geometry, the C_2 axes go through the C and Li atoms. A NBO analysis was performed for this system in order to describe its electronic structure. Filled NBOs describe the different bonds or lone pairs that correspond to an idealized "strictly" localized Lewis structure. The real system deviates from this hypothetical structure because of donor−acceptor interactions between filled and empty NBOs. It thus provides a measure of the energetics of delocalization/hyperconjugation. As expected, the NBO analysis indicates that the S−Li and C−Li interactions are essentially electrostatic in nature ($n_{Wiberg} < 0.1$, $q_{Li} > 0.8$). It also points to a Lewis structure which involves two lone pairs at the carbon center, three lone pairs at each sulfur atom, and single P−C and P−S bonds. The two lone pairs at the carbon center are described by two nonequivalent NBOs that possess different hydridization and energies. The lowest one (LP1(C)) is an sp^2-hybridized orbital ($sp^{2.17}$) and lies in the PCP plane, whereas the second one (LP2(C)) is a pure p orbital (Table 2 and Figure 5), perpendicular to the PCP plane.

These orbitals strongly contribute to the highest occupied molecular orbitals of the Kohn−Sham orbital diagram. For example, the HOMO of the system is mainly a b3 symmetry combination of the carbon p orbitals (LP2(C)), whereas HOMO-2 consists of an antibonding interaction of the two LP1(C) NBOs (Figure 5).

The NBO charge analysis is consistent with the Lewis structure (Table 2) with a highly charged carbon center ($q_c = -1.77$) and both charged sulfur ($q_s = -0.80$) and phosphorus centers ($q_p = +0.91$). The Wiberg bond indexes for both P−C and P−S bonds reveal a single-bond character (1.19 and 1.10, respectively). This should be compared to the Wiberg bond index calculated for the phosphaalkene HP═CH_2 of 1.96 (same level of theory), in which a genuine double bond is involved. Though very short P−C bond distances are both measured in **A** and in HP═CH_2 (1.687 and 1.673 Å, respectively), the P−C bonding scheme in these systems differs remarkably: no P−C double-bond character is involved in **A** (in terms of p_π/d_π interaction).[55−59] However, in system **A** the carbon lone pairs are involved in donor−acceptor interactions: i.e. donation from LP1(C) and LP2(C) to the six vicinal antibonding σ^*(P−S) and σ^*(P−H). This hyperconjugation results in very significant stabilization of the carbon lone pairs without involvement of P−C double-bond character.

The resulting interaction energy can be estimated via either deletion of the appropriate off-diagonal elements of the Fock matrix in the NBO basis (E_{del} energy) or standard second-order perturbation approach (that affords a $E(2)$ energy). The magnitude of the donor−acceptor interaction is mainly controlled by (i) the energy gap (ΔE_{ij}) between the donor and acceptor orbitals, (ii) the corresponding Fock matrix element F_{ij}, and (iii) the occupation of the donor orbital n_i. As shown in Table 3, the filled LP1(C) behaves as donor orbital and interacts with the two vicinal σ^*(P−S) (Figure 6) and the four σ^*(P−H) orbitals (Figure 6) with similar magnitudes (3.59−5.54 kcal mol^{-1} ($E(2)$)). As expected for stereoelectronic effects, stabilization of the carbon lone pairs by the vicinal antibonding σ^* orbitals strongly depends on the relative orientation of the donor/acceptor orbitals. Thus, as the two σ^*(P−S) orbitals lie in the PCP plane, i.e. in the LP2(C) nodal plane, LP2(C) cannot be stabilized by them. LP2(C) is, however, stabilized by the four vicinal σ^*(P−H) orbitals. Each vicinal σ^*(P−H) orbital contributes by over 11 kcal mol^{-1} to the $E(2)$ energy (11.99−16.86 kcal mol^{-1} each). Indeed, the LP2(C) orbital is a nonhybridized higher energy p orbital; this makes this lone pair a stronger donor and leads to a decreased energy gap ΔE_{ij} (0.35 au for LP2(C)→σ^*(P−H) compared to 0.47 au for LP1(C)→σ^*(P−H)). Greater overlaps develop between LP2(C) and σ^*(P−H)

(53) Becke, A. D. *J. Chem. Phys.* **1993**, *98*, 5648.
(54) Perdew, J. P.; Wang, Y. *Phys. Rev. B* **1992**, *45*, 13244.
(55) Ruben, E. A.; Chapman, M. S.; Evanseck, J. D. *J. Am. Chem. Soc.* **2005**, *127*, 17789.
(56) Cramer, C. J. *J. Mol. Struct. (THEOCHEM)* **1996**, *370*, 135.
(57) Koch, R.; Anders, E. *J. Org. Chem.* **1995**, *60*, 5861.
(58) Kranz, M.; Denmark, S. E. *J. Org. Chem.* **1995**, *60*, 5867.
(59) Gilheany, D. G. *Chem. Rev.* **1994**, *94*, 1339.

Chart 2

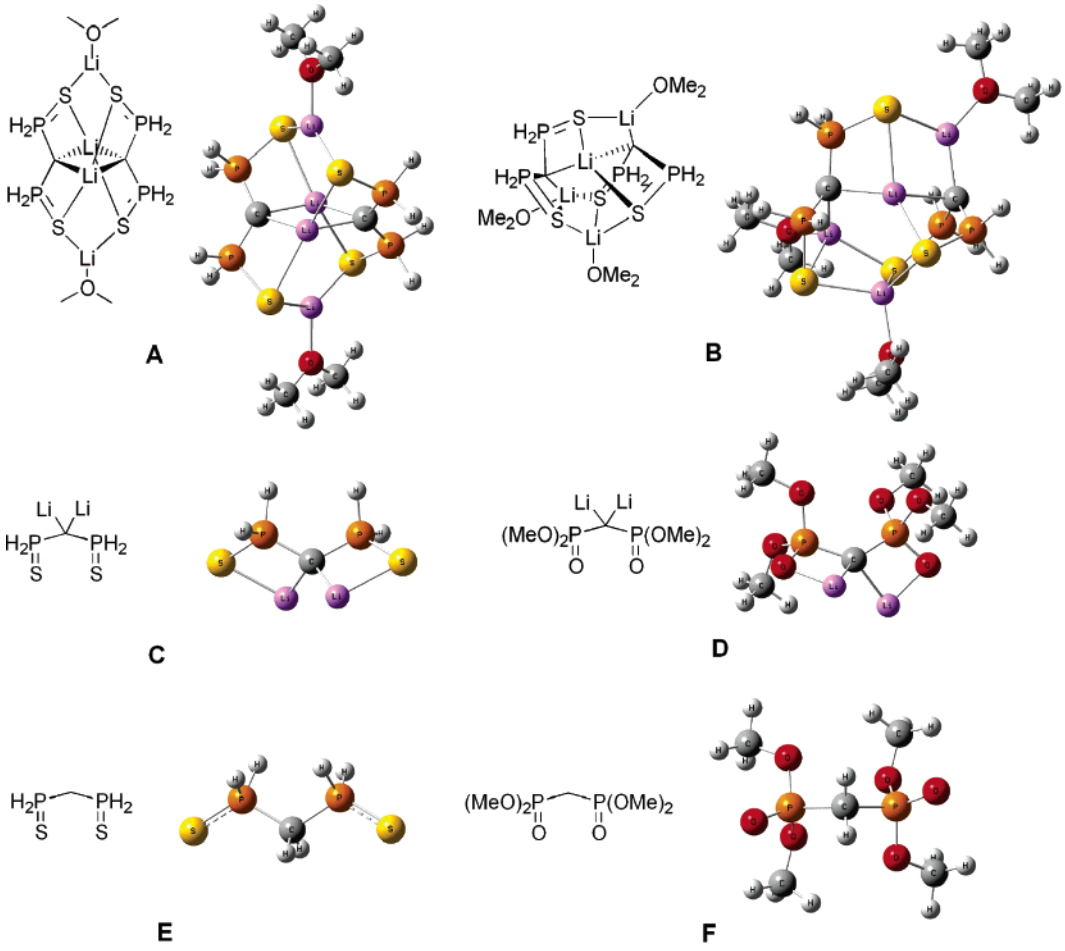

Table 1. Structural Comparison of 1,[47] 2A, 2B, and A−F

	P−C, Å		P−X, Å		C−Li, Å		P−C−P, deg	X−P−C−P, deg	
1 (X = S)	1.827	1.831	1.948	1.941			118.4	61.3	47.3
2A (X = S)	1.672(3)	1.678(3)	2.037(1)	2.040(1)	2.195(5)	2.159(5)	131.6(2)	160.3	174.3
	1.676(3)	1.678(3)	2.039(1)	2.041(1)	2.196(5)	2.173(5)	131.3(2)	167.2	171.4
2B (X = S)	1.681(2)	1.693(2)	2.048(2)	2.036(1)	2.343(4)	2.120(4)	120.6(1)	73.4	63.2
	1.683(2)	1.685(2)	2.032(1)	2.038(1)	2.181(4)	2.200(4)	130.6(1)	103.8	179.2
A (X = S)	1.687		2.048		2.174		126.5	172.2	
B (X = S)	1.689	1.696	2.061	2.04	2.108	2.135	126.5	102.1	173,0
	1.702	1.71	2.067	2.053	2.068	2.282	114.9	88.2	59,0
C (X = S)	1.718	1.718	2.035	2.035	2.048	2.048	122.6	138.3	138.3
D (X = O)	1.694	1.694	1.542	1.542	2.068	2.068	127.5	155.2	154.3
E (X = S)	1.84	1.848	1.95	1.95			114.67	51.16	170.96
F (X = O)	1.819	1.82	1.486	1.486			122,0	163.7	163.3

Table 2. NBO Analysis of A−F

	NBO charge					Wiberg bond index				lone pair of C			
		q_P		q_X	q_{Li}	n(P−C)	n(P−X)	n(P−R)		hybridizn		pop.	
	q_C									LP1	LP2	LP1	LP2
A (R = H, X = S)	−1.77	0.91		−0.80	0.80 0.84	1.19	1.10	0.84	0.85	$sp^{2.17}$	$p^{1.00}$	1.74	1.63
B (R = H, X = S)	−1.73	0.87	0.90	−0.79 −0.84	0.86 0.77	1.21 1.17	1.03 1.09	0.86 0.89	0.89 0.86	$sp^{2.43}$	$p^{1.00}$	1.74	1.64
	−1.79	0.91	0.91	−0.83 −0.79	0.86 0.80	1.20 1.17	1.12 1.07	0.84 0.85	0.87 0.87	$sp^{1.84}$	$p^{1.00}$	1.75	1.61
C (R = H, X = S)	−1.88	0.88		−0.76	0.86	1.13	1.16	0.87	0.85	$sp^{2.11}$	$p^{1.00}$	1.79	1.68
D (R = OMe, X = O)	−2.01	2.37		−1.23	0.93	1.15	1.03	0.66	0.69	$sp^{3.74}$	$p^{1.00}$	1.78	1.67
E (R = H, X = S)	−1.19	0.79		−0.54		0.84	1.43	0.87	0.87				
F (R = OMe, X = O)	−1.31	2.41		−1.08		0.81	1.28	0.70	0.71				

NBOs that result in higher F_{ij} and $E(2)$ values. The Kohn−Sham orbitals illustrate the participation of antibonding σ^*(P−H) and σ^*(P−S) orbitals in the stabilization of the carbon lone pairs: the HOMO, for example, exhibits non-negligible coefficients on hydrogen and phosphorus centers that show a stabilizing interaction between an appropriate combination of σ^*(P−H) orbitals and the carbon p orbital.

These donor−acceptor interactions finally lead to a stabilization of both carbon lone pairs by hyperconjugation (to the six vicinal σ^*(P−H) and σ^*(P−S) NBOs). LP1(C) is stabilized by

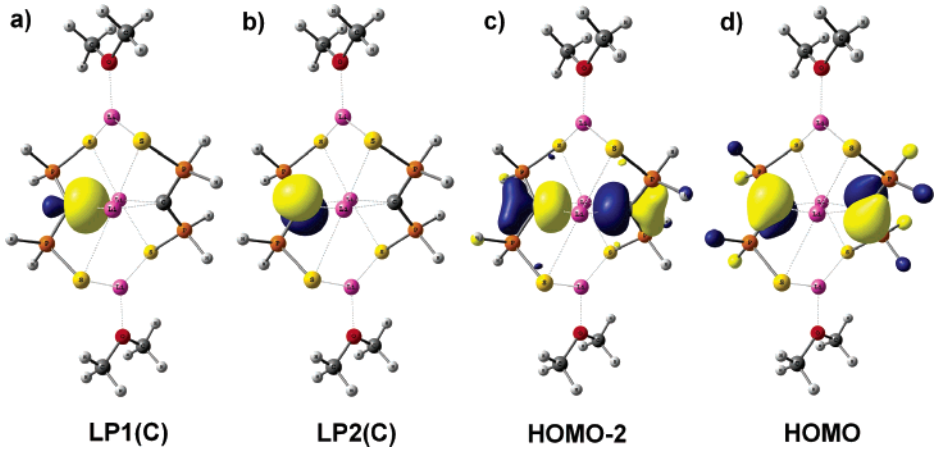

Figure 5. NBOs and Kohn−Sham orbitals involving the carbon lone pairs in **A**: (a) NBO plot of LP1(C) ($sp^{2.17}$); (b) NBO plot of LP2(C) (p); (c) HOMO-2; (d) HOMO.

Table 3. NBO Analysis of Hyperconjugative Interactions in A (for One Monomer)

orbital		$E(2)$		
donor	acceptor	(kcal mol^{-1})	ΔE_{ij} (au)	F_{ij} (au)
LP1(C) $sp^{2.17}$	1 σ^*(P−S)	3.73	0.38	0.036
LP1(C) $sp^{2.17}$	1 σ^*(P−H)	5.54	0.47	0.047
LP1(C) $sp^{2.17}$	1 σ^*(P−H)	3.59	0.47	0.038
LP2(C) p	1 σ^*(P−S)	<0.5		
LP2(C) p	1 σ^*(P−H)	11.99	0.36	0.062
LP2(C) p	1 σ^*(P−H)	16.86	0.35	0.073

orbital		E_{del}[a]
donor	acceptor	(kcal mol^{-1})
LP1(C) $sp^{2.17}$	2 σ^*(P−S) + 4 σ^*(P−H)	33.8
LP2(C) p	2 σ^*(P−S) + 4 σ^*(P−H)	65.5
LP1(C) $sp^{2.17}$ + LP2(C) p	2 σ^*(P−S) + 4 σ^*(P−H)	110.7

[a] Energy of deletion.

33.8 kcal mol^{-1} (estimated by deletion of the six LP1(C)→σ^*-(P−H,S) elements of the Fock matrix) and LP2(C) by 65.5 kcal mol^{-1}; the total stabilization energy is over 110 kcal mol^{-1} (per monomer).

These results account for the structural modifications observed between the neutral species **E** and the dianionic system **A**. In particular, a shortening of the P−C bonds (from 1.840 Å in **E** to 1.687 Å in **A**) with a concomitant elongation of the P−S bonds are noticed upon double deprotonation. These changes are due to negative hyperconjugation (vide supra) that strengthens the P−C interaction and weakens the P−H and P−S bonds in **A**. In **E** short P−S bonds are observed, due to negative hyperconjugation of the types LP(S)→σ^*(P−C) and LP-(S)→σ^*(P−H).[59] However increase of the electronic density on the carbon atom in **A** (q_C = −1.19 in **E** vs −1.77 in **A**) decreases the acceptor ability of the σ^*(P−C) orbital (note that $\Delta E_{LP(S)\rightarrow\sigma^*(P-C)}$ varies from 0.35 au in **E** to 0.52 au in **A**). Together with the LP1(C)→ σ^*(P−S) interaction it thus destabilizes the P−S bonds (n_{Wiberg}=1.43 in **E** vs 1.1 in **A**) and increases the charge at the sulfur atoms (q_S=-0.54 in **E** vs −0.80 in **A**).

It was evidenced by NMR spectroscopy that, in solution, the dimeric structure **2A** found in the solid state is not preserved and another aggregate forms at low temperature which very likely exhibits a structure close to **2B** (vide supra). The dimeric lithium salt **B** was thus investigated by DFT calculations. As depicted in Tables 1 and S1 (presented in Supporting Information), the aggregate has a significant impact neither on the structural parameters nor on the NBO analysis. As noted previously, the magnitude of the hyperconjugative interaction has been evaluated by deletion of the off-diagonal elements in the Fock matrix. The analysis revealed here also that LP1(C) is less stabilized than LP2(C) upon interaction with the vicinal σ^*(P−S) and σ^*(P−H) NBOs (sum 25.1 (av) kcal mol^{-1} and 56.4 (av) kcal mol^{-1}, respectively). The major geometrical alteration is due to the P−C−P−S dihedral angles, which vary from 172.2° in **A** (sulfur atoms almost belong to the PCP plane) to 59.0−173.0° in nonsymmetrical **B** (which possess two markedly different dianionic fragments). With this geometry, the empty σ^*(P−S) NBO can participate in the stabilization of LP2(C). In any event, the overall stabilization energy corresponding to LP1(C)+LP2(C)→$\sigma^*_{vicinal}$ hyperconjugation interactions is not affected by this redistribution of the donor−acceptor interactions (103.2 vs 110.7 kcal mol^{-1} in **A**).

These results are in line with the low rotation energy known for phosphorus ylides. Indeed, we evaluated the corresponding energy barrier for rotation of the P−S arms around the P−C bonds on the free dianion $(H_2PS)_2C^{2-}$ to fall below 3 kcal mol^{-1}.

DFT Calculations: Comparison between Dianions 2 and 6. It was shown above that the state of aggregation of the dianion **2** does not lead to significant modifications of the structural parameters and the NBO analysis. Moreover, the insolubility of dianion **6** clearly points to a polymeric arrangement, whose structure can therefore not be postulated. As a consequence, to compare the electronic situations of the two types of dianions, the monomeric model compounds **C** and **D** were computed. Geometries of the models were optimized as dilithium salts in point group C_2 (the C_2 axis being the bisector of the PCP angle), and the structural parameters are summarized in Table 1. These are in agreement with the previously studied models **A** and **B**: i.e., short P−C bonds and long P−O (respectively P−S) bonds. NBO analyses were performed to precisely determine the electronic distribution in **C** and **D** (Table S2; see the Supporting Information).

The hyperconjugation energy (evaluated via $E(2)$ or E_{del}) in **C** differs significantly from that calculated in dimers **A** and **B** (83.2 kcal mol^{-1} in **C** vs 106.5 (av) kcal mol^{-1} in dimers). This difference is due to the unsaturation of the coordination sphere at the lithium centers in **C**. Indeed, it results in a stronger interaction of the lithium cations with the carbon and sulfur atoms in nonsolvated **C** than in **A** or **B** (for example: C−Li = 2.048 Å in **C** vs 2.16 (av) Å in **A** and **B** and 2.20 (av) Å in experimental structures **2A** and **2B**). This noticeably deforms the C−P−S−Li four-membered rings and in particular elongates the P−C bonds (P−C = 1.718 Å in **C** vs 1.69 (av) Å in **A** and

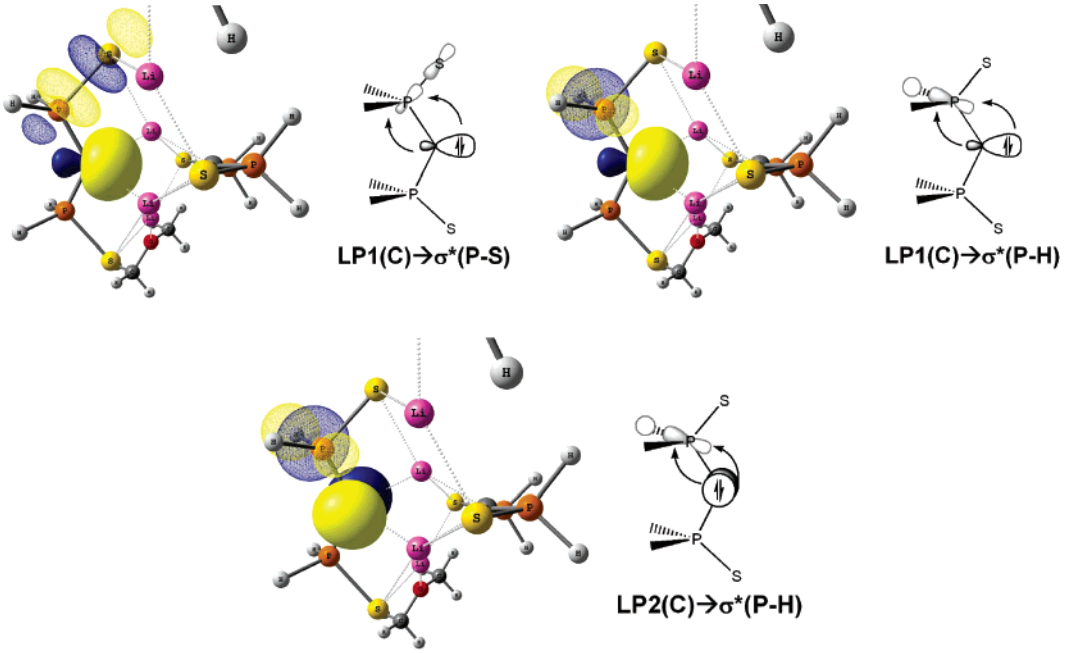

Figure 6. NBO plots of principal donor−acceptor interactions in **A**. Empty acceptor NBOs are represented by a mesh surface and filled donor NBOs by a solid surface.

B and 1.68 (av) Å in experimental structures **2A** and **2B**); it finally leads to a decrease of the hyperconjugative interactions. We can therefore not directly compare the nonsolvated lithium salt **C** with **A** and **B**; however, **C** and **D** can be compared to evaluate the differences between the bis(thiophosphinoyl) and bis(phosphonate) systems.

As expected, in the dianionic system **D**, the carbon center bears two nonequivalent lone pairs. LP1(C) is an $sp^{3.74}$-hybridized orbital, whereas LP2(C) is a pure p orbital. This situation slightly differs from that observed for the bis(thiophosphinoyl) models **A**−**C**, for which LP1(C) is almost sp^2-hybridized. The higher p character found in LP1(C) in **D** increases its donor ability since it raises its energy and maximizes the size of its back lobe, responsible for a greater overlap with acceptor NBOs. In fact, the energy gaps (ΔE_{ij}) calculated for LP1(C)→σ*(P−O) and LP1(C)→σ*(P−OMe) fall in the range of the related energy gaps observed for **C**. Moreover, σ*(P−O) and σ*(P−OMe) orbitals are strongly polarized toward phosphorus (up to 79% contribution at P) due to the higher electronegativity of oxygen. Overall, these two factors lead to an increased overlap between donor LP1(C) and acceptor σ*(P−O) and σ*(P−OMe), yielding a greater stabilization of LP1(C) in **D** (E_{del} = 36.0 kcal mol^{-1}) than in **C** (E_{del} = 24.6 kcal mol^{-1}). As far as LP2(C) stabilization is concerned, similar energy gaps between this donor NBO and vicinal empty σ* NBOs in **D** and **C** were calculated (Table S2). Then, because of the polarization of the σ*(P−O) orbitals toward P, greater overlaps develop in **D** that lead to increased F_{ij} terms and, thus, to a greater stabilization of LP2(C) for the bis(phosphonate) derivative (E_{del} = 77.6 kcal mol^{-1} in **D** vs 52.6 kcal mol^{-1} in **C**). The bis(phosphonate) backbone finally allows a greater stabilization of the carbon lone pairs than the bis(thiophosphinoyl) backbone, the total energy deletion (corresponding to the 12 elements of the Fock matrix: LP1(C)→ $\sigma^*_{vicinal}$ and LP2(C)→$\sigma^*_{vicinal}$) being 121.5 kcal mol^{-1} for **D** and 83.2 kcal mol^{-1} for **C**. Attention must be paid that this difference does not result in a decrease of the electron density at the carbon center in **D**: the populations of LP1(C) and LP2(C) in **C** and **D** are equal (1.78 for LP1(C) and 1.67 for LP2(C)). Moreover, the same structural modifications are found between the neutral species

Scheme 7

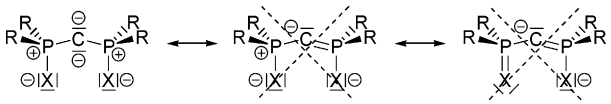

(**E**, **F**) and their dianionic equivalents (**C**, **D**): i.e., a shortening of the P−C bonds concomitant with an elongation of the P−X bonds occurs upon double deprotonation.

According to this analysis, the dianionic species **2** and **6** are best described by the Lewis structure drawn in Scheme 7. The central carbon atom bears two nonequivalent lone pairs strongly stabilized by negative hyperconjugation (i.e. donation to the vicinal antibonding P−R and P−X bonds). This leads to very short P−C bonds without involvement of double-bond character. Moreover, these hyperconjugation interactions preferentially stabilize the best donor orbitals (i.e. LP(C)). This results in a decreased stabilization of the X-substituent lone pairs (LP(S) and LP(O)) and, thus, in an increased negative charge at the X centers (concomitant with an elongation of the P−X bonds). Finally, delocalization forms that involve P−X or P−C double bonds are not accurate to describe the stability of such systems, since they would involve a p_π−d_π bonding scheme abandoned for over 10 years.[59]

Reactivity toward CS_2. The coordination chemistry of 1,1-ethylenedithiolato ligands has mostly been developed with late-transition-metal centers, such as Ni, Pd, Pt, Cu, and Au.[60−64] Among these complexes, some display interesting properties, such as luminescence in the cases of Pt(II) and Au(I) complexes. The ready access of the aforementioned dianions led us to explore their reaction with CS_2 in order to obtain a new class of such 1,1-ethylenedithiolato ligands (Scheme 8).

(60) Vicente, J.; Chicote, M. T.; Gonzalez-Herrero, P.; Jones, P. G.; Humphrey, M. G.; Cifuentes, M. P.; Samoc, M.; Luther-Davies, B. *Inorg. Chem.* **1999**, *38*, 5018.
(61) Zuleta, J. A.; Burberry, M. S.; Eisenberg, R. *Coord. Chem. Rev.* **1990**, *97*, 47.
(62) Zuleta, J. A.; Chesta, C. A.; Eisenberg, R. *J. Am. Chem. Soc.* **1989**, *111*, 8916.
(63) Hanna, S. D.; Zink, J. I. *Inorg. Chem.* **1996**, *35*, 297.
(64) Hollande, F.; Caffery, M. L.; Coucouva. D. *J. Am. Chem. Soc.* **1974**, *96*, 6, 4682.

Scheme 8

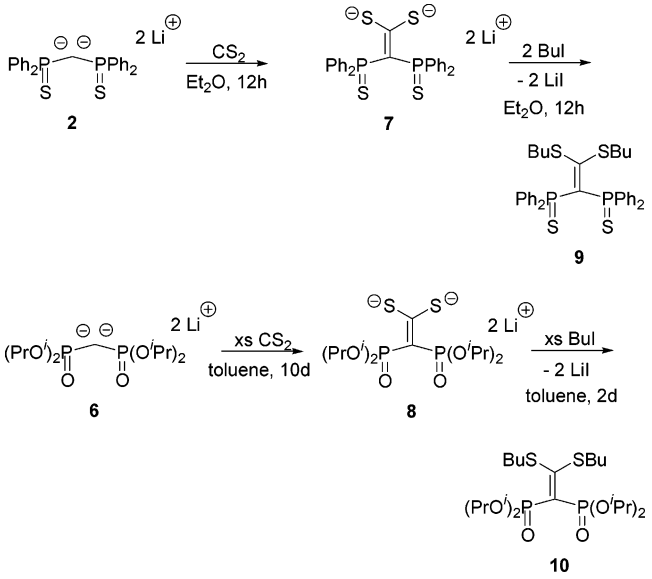

As noted for the synthesis of the dianions **2** and **6**, their reactivities were very different in terms of kinetics. Indeed, reaction of the dianion **2** with a stoichiometric amount of CS_2 at room temperature for 12 h led to the formation of a yellow precipitate in an excellent yield of 95%. This species, **7**, is partially soluble in THF and more so in pyridine, which allowed a full spectral analysis. Compound **7** was also characterized by elemental analyses. On the other hand, the reaction of dianion **6** with CS_2 required a 10-fold excess of CS_2 for 10 days to go to completion. Compound **8**, which was isolated as a yellow solid, is soluble in C_6D_6 and was thus fully characterized by the usual NMR techniques as well as elemental analyses. In turn, these new dianionic ligands, the 1,1-ethylenedithiolates **7** and **8** were reacted with butyl iodide to yield the air-stable neutral species **9** and **10** quantitatively. Both species were isolated as yellow solids and fully characterized by NMR as well as elemental analyses. Concerning the bis(thiophosphinoyl) derivatives, a downfield chemical shift of 15 ppm is observed in the ^{31}P NMR spectrum on going from **2** to **7**. Upon alkylation, forming compound **9**, a minor change was observed: from 38 to 41 ppm. Most interestingly, in the ^{13}C NMR spectrum of **7**, the signal for the ethylenic $C(P_2)$ moiety appears as the expected triplet ($^1J_{C-P}$ = 93.5 Hz) at high field (δ 87.8 ppm). The ethylenic $C(S_2)$ moiety also appears as a triplet ($^2J_{C-P}$ = 5.2 Hz), but at very low field (δ 225.3 ppm). This points to a very large partial charge difference between these two carbon centers. In the neutral species **9**, the two chemical shifts are found at 125.7 ppm ($^1J_{C-P}$ = 64.5 Hz) and 175.9 ppm ($^2J_{C-P}$ = 2.7 Hz), respectively. In the case of the bis(phosphonate) derivatives **8** and **10**, the CP_2 moiety could not be observed in the ^{13}C NMR spectrum, but the chemical shifts for the ethylenic $C(S_2)$ moieties were found (at δ 227.4 and 183.7 ppm, respectively). Attempts were made to crystallize these species in order first to obtain structural information and possibly to correlate the chemical shifts to geometrical features of the newly formed double bonds. Crystals of dianion **7** and of compound **9** were obtained by a slow diffusion of hexane in a pyridine solution of **7** and a CH_2Cl_2 solution of **9**. The structures of **7** and **9** are presented in Figures7 and 8. Information concerning the data collection and refinement are given in the Supporting Information for both compounds.

Compound **7** crystallized as a C_2-symmetrical dimer. It shows two different tetrahedral arrangements for the lithium cations.

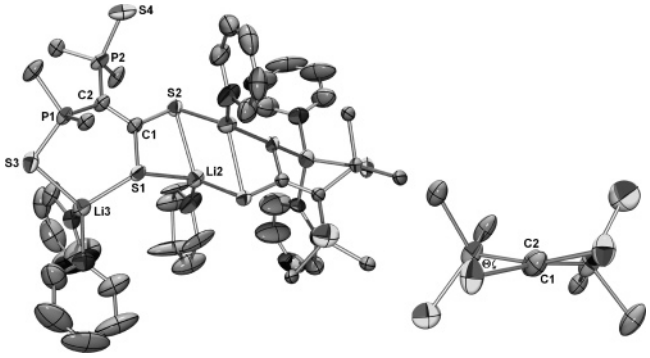

Figure 7. View of one molecule of **7** (thermal ellipsoids set at 50% probability). The hydrogen atoms and phenyl rings are omitted for clarity. The partial structure on the right side illustrates the θ twist angle. Selected bond lengths (Å) and angles (deg): C1−C2 = 1.401(2), C2−P1 = 1.786(2), C2−P2 = 1.783(2), C1−S1 = 1.736(2), C1−S2 = 1.733(2), P1−S3 = 1.984(1), P2−S4 = 1.955(1); P1−C2−P2 = 122.5(1), S1−C1−S2 = 115.9(1). θ = 12.6, 18.1.

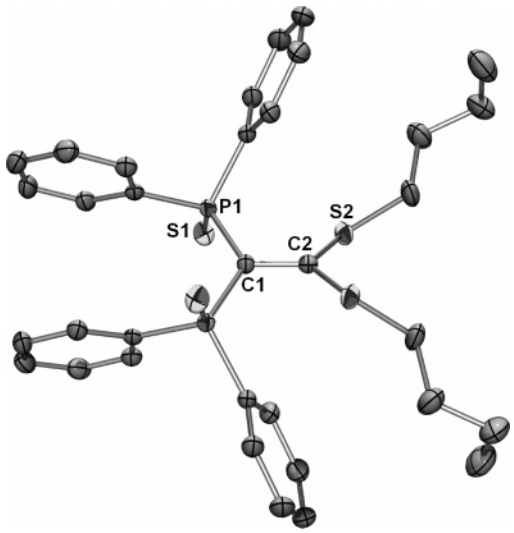

Figure 8. View of one molecule of **9** (thermal ellipsoids set at 50% probability). The hydrogen atoms are omitted for clarity. Selected bond lengths (Å) and angles (deg): C1−C2 = 1.378(3), C1−P1 = 1.818(1), C2−S2 = 1.738(1), P1−S1 = 1.956(1); P1−C1−P1′ = 123.6(1), S2−C2−S2′ = 120.4(1).

In each unit of the dimer, one lithium (Li3) binds the two sulfur atoms of the CS_2 moiety and its coordination sphere is completed by two molecules of pyridine. The other lithium atom (Li2) is bound to three sulfur centers (S1 and S2 of the subunit, and a sulfur atom of the other dianionic unit). The two thiophosphinoyl moieties are different. Indeed, S3 is not bound to a lithium center, whereas S4 is bound to Li3. S1 is bound to both Li2 and Li3, which belong to the same dianionic unit of the dimer, and S2 is bound to Li2 and to the lithium center of the second unit. In terms of metric parameters, the C1−C2 bond distance is quite long (1.401(2) Å), whereas the C−S bonds are rather short (C1−S1 = 1.736(2) Å, C1−S2 = 1.733(2) Å). In fact, in comparison to the neutral bis(thiophosphinoyl)-methane **1**, the P−C bond distances are short (C2−P1 = 1.786-(2) Å, C2−P2 = 1.783(2) Å) and the P−S bonds are long (P1−S3 = 1.984(1) Å, P2−S4 = 1.955(1) Å). Moreover, a large twist is observed for the newly formed double bond: θ = 15.3° (Figure 7). The structure of the neutral species **9** presents a few peculiar features. An even larger twist of the double bond is noted (SCCP dihedral angle of 22.2°).[49] In comparison to dianion **7**, the C1−C2 bond distance is shorter (1.378(3) Å)

Table 4. Structural Parameters and NBO Analysis for G−J and TSG−TSJ

	structural parameters						
	C1−C2	C2−P	C1−S	P−X	θ	P−C2−P	S−C1−S
G (X = S)	1.437	1.768	1.729	2.018	5.9	115.2	123.5
H (X = S)	1.361	1.826	1.772	1.955	11.8	114.9	120.3
I (X = O)	1.477	1.745	1.717	1.5	40.1	121.1	123.3
J (X = O)	1.372	1.817	1.761	1.488	32.3	120.4	120.8
TSG (X = S)	1.508	1.73 (av)	1.70 (av)	2.02 (av)	88.4	121.4	124.5
TSH (X = S)	1.426	1.78 (av)	1.71 (av)	1.97 (av)	83.2	121.0	134.9
TSI (X = O)	1.502	1.74 (av)	1.71 (av)	1.50 (av)	61.7	121.2	122.9
TSJ (X = O)	1.449	1.752	1.696	1.495	90.2	128.3	134.9

	NBO charge				Wiberg bond index			C1=C2 π bond polarization	
	q_{C1}	q_{C2}	q_X	q_S	C1−C2	C1−S	C2−P	% C1	% C2
G (X = S)	−0.28	−1.08	−0.77	−0.4	1.27	1.73	0.95	27.9	72.1
H (X = S)	−0.34	−0.78	−0.54	0.32	1.71	1.08	0.83	46.1	53.9
I (X = O)	−0.29	−1.26	−1.12	−0.36	1.13	1.72	0.97	40.1	59.9
J (X = O)	−0.32	−0.94	−1.09	0.34	1.64	1.11	0.79	43.9	56.1
TSG (X = S)	−0.34	−1.19	−0.78	−0.3	1.01	1.71	1.03		
TSH (X = S)	−0.31	−1.18	−0.57	0.50	1.16	1.31	0.87		
TSI (X = O)	−0.32	−1.28	−1.12	−0.33	1.07	1.45	0.99		
TSJ (X = O)	−0.24	−1.31	−1.11	0.54	1.11	1.38	0.86		

and the P−C bond distances are longer (C2−P1 = 1.818(1) Å) and fall in the range of the P−C bond distances in **1**. The most significant differences between these two species will be rationalized below in light of DFT calculations on model compounds.

DFT Calculations: Electronic Structures of the Double-Bonded Compounds. In order to gain information not only on the electronic structures of compounds **7** and **9** but also on the bis(phosphonate) derivatives **8** and **10**, DFT calculations were performed on the model compounds **G**−**J** (Chart 3).

Chart 3

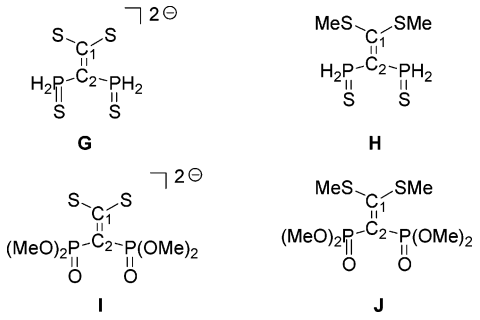

Optimized geometries are in good agreement with the experimental structures obtained for **7** and **9**. In particular, long C=C bond distances are measured, being over 1.43 Å in the dianionic species **G** and **I** (1.437 and 1.477 Å, respectively) and 1.35 Å in the neutral species **H** and **J** (1.361 and 1.372 Å, respectively). As noted in the X-ray structures, the C=C double bond is twisted in the four compounds **G**−**J**; the corresponding dihedral twist angles vary from 5.9 to 40.1° (see Table 4). These features clearly indicate that a weak C=C bond is involved in dianions **G** and **I** and to a lower extent in neutral compounds **H** and **J**. The rotation energy barriers corresponding to the isomerization of the C=C double bond (where the CS_2 group is perpendicular to the PCP moiety) have been evaluated via both a singlet and a triplet pathway. In all cases the singlet isomerization process is favored by over 14 kcal mol^{-1} and requires a very low energy, especially for the dianions (17.5 kcal mol^{-1} for **G**, 32.9 kcal mol^{-1} for **H**, 4.8 kcal mol^{-1} for **I**, and 25.2 kcal mol^{-1} for **J**). NBO analyses were performed to clarify the electronic distribution in dianions **G** and **I**. As expected, the Wiberg bond index for the C=C bond is low for a C=C double bond in both **G** and **I** (1.20 (av)), even lower than in neutral species **H** and **J** (1.68 (av)) and only slightly higher than in transition states **TSG** and **TSI** (1.04 (av)), for which no C=C π overlap can develop. Moreover, the NBO describing the C=C π bond is strongly polarized toward C_2 (i.e. PCP). For example, in **G**, the C1=C2 π bond is a combination of the C2 p_z orbital, which contributes 72.1% to the π bond, and the C1 p_z orbital (27.9%). This results in an increased negative charge on the C2 center (NBO charge $q_{C2} = -1.08$ vs $q_{C1} = -0.28$ for C_1 in **G**, compared to $q_{C2} = -0.79$ and $q_{C1} = -0.34$ in **H**).

Scheme 9

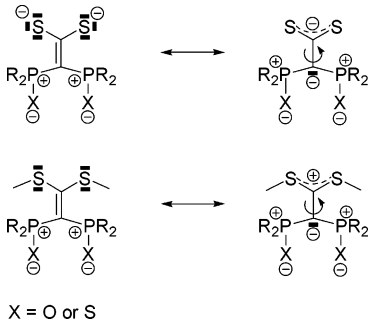

The C=C bond polarization in dianions **G** and **I** (and to a lower extent in **H** and **J**) is due to the substitution scheme of the double bond. Indeed the thiolato substituents at the C1 carbon behave as π donor groups that stabilize an electropositive carbon center. It leads to short S−C1 bonds and increased S−C1 Wiberg bond indexes (see Table 4). On the other hand, the P^V substituents are able to stabilize a negative charge on the C2 center by negative hyperconjugation and thus behave as acceptor groups. Short P−C1 and long P−S (or P−O) bonds together with the presence of a negative charge on C1 are diagnostic of stabilization interactions by hyperconjugation (Table 4). This "push−pull" system polarizes the C1=C2 double bond; compounds **G**−**J** are thus best described by two delocalized forms (Scheme 9).[49]

These forms in particular account for the low rotation barrier around the C1=C2 bond since the transition states are strongly stabilized by the four substituents. In particular, the greater donor ability of the thiolato substituents decreases the energy barrier for dianions **G** and **I** compared to **H** and **J**.

Conclusion

We have presented here a full description, structural and electronic, of **2**, the geminal dianionic bis(thiophosphinoyl) species that we have recently developed. The synthesis and characterization of the first geminal dianion of a bis(phosphonate) derivative **6** was also reported. The two different X-ray structures obtained for dianion **2** as well as the variable-temperature ^{7}Li and ^{31}P NMR experiments clearly show that the state of aggregation of these polyanionic compounds in solution or the solid state can vary to a great extent with little external stimulus. The electronic structure of these uncommon species has been described on the basis of DFT calculations. It indicates that both thiophosphinoyl and phosphonate groups are efficient for the stabilization of a dianionic carbon center via negative hyperconjugation. These donor−acceptor interactions were studied by means of NBO analysis; they result in short P−C bonds without involvement of double-bond character and increased negative charge at the sulfur centers. Trapping of these species with CS_2 afforded a new class of ethylenedithiolate ligands (**7** and **8**) that present strongly polarized C═C double bonds. The solid-state structure obtained for **7** revealed that these new dianionic tetradentate ligands possess various coordination modes. The coordination chemistry of these new dianionic species (**2** and **6**−**8**) is currently being pursued.

Experimental Section

General Remarks. All reactions were routinely performed under an inert atmosphere of argon or nitrogen by using Schlenk and glovebox techniques and dry deoxygenated solvents. Dry THF, ether, and hexanes were obtained by distillation from Na/benzophenone. Dry dichloromethane was distilled on P_2O_5 and dry toluene on Na. Nuclear magnetic resonance spectra were recorded on a Bruker AC-300 SY spectrometer operating at 300.0 MHz for ^{1}H, 75.5 MHz for ^{13}C, and 121.5 MHz for ^{31}P. Solvent peaks are used as internal references relative to Me_4Si for ^{1}H and ^{13}C chemical shifts (ppm); ^{31}P chemical shifts are relative to an 85% H_3PO_4 external reference. Coupling constants are given in hertz. The following abbreviations are used: s, singlet; d, doublet; t, triplet; m, multiplet; v, virtual. Elemental analyses were performed by the "Service d'analyze du CNRS", at Gif sur Yvette, France. All reagents and chemicals were obtained commercially and used as received.

Computational Details. All calculations were carried out using the Gaussian 03W package.[65] Geometry optimizations were carried out at the B3PW91 level of theory.[53,54] H, Li, C, O, P, and S atoms were represented by the 6-31+G* basis set. Model compounds were obtained by replacing phenyl groups by hydrogen atoms and alkyl groups by methyl substituents. Electronic structures of these model compounds were studied using natural bond orbital (NBO) analysis, by means of the NBO 3.0 program interfaced into the Gaussian program. The NBO analysis transforms the canonical delocalized Hartree−Fock (HF) molecular orbitals (MOs) into localized orbitals that are closely tied to chemical bonding concepts (core atomic orbitals, bonds, and nonbonding lone pairs). This process involves sequential transformation of nonorthogonal atomic orbitals (AOs) to the sets of "natural" atomic orbitals (NAOs), hybrid orbitals (NHOs), and bond orbitals (NBOs). Each of these localized basis sets is complete and orthonormal. Filled NBOs describe bonds or lone pairs and thus refer to the hypothetical strictly localized Lewis structure. The interactions between filled and antibonding (or Rydberg) orbitals represent the deviation of the molecule from the idealized Lewis structure and can be used as a measure of delocalizations. Since the occupancies of filled NBOs are highly condensed, the delocalizing interactions can be treated by a standard second-order perturbation approach (referred to as $E(2)$ energies) or by deletion of the corresponding off-diagonal elements of the Fock matrix in the NBO basis (referred to as E_{del} energies). Detailed descriptions of the NBO calculations are available in the literature.

X-ray Structure Data. Details of the refinement are as follows: Nonius KappaCCD diffractometer, ϕ and ω scans, Mo Kα radiation ($\lambda = 0.710\ 73$ Å), graphite monochromator, $T = 150$ K, structure solution with SIR97,[66] refinement against F^2 in SHELXL97[67] with anisotropic thermal parameters for all non-hydrogen atoms, calculated hydrogen positions with riding isotropic thermal parameters.

Crystallographic data for the structures reported in this paper have been deposited with the Cambridge Crystallographic Data Centre as Supplementary Publication Nos. CCDC 603109−603112. Copies of the data can be obtained free of charge on application to the CCDC, 12 Union Road, Cambridge CB2 1EZ, U.K. (fax, (+44)-1223-336-033; e-mail, deposit@ccdc.cam.ac.uk).

Synthesis of 1. The procedure reported in ref 68 was modified as follows: to a suspension of bis(diphenylphosphino)methane (6.00 g, 15.6 mmol) in THF (20 mL) was added 2 equiv of elemental sulfur (0.25 equiv of S_8: 1.00 g, 3.9 mmol) at room temperature. The resulting solution was stirred for 3 h at 60 °C. Pure **2** was finally obtained as a white solid after evaporation of the solvents. Yield: 100% (7.00 g, 15.6 mmol). Selected data: ^{31}P{^{1}H} NMR (121.5 MHz, $CDCl_3$, 25 °C, 85% H_3PO_4 as external standard) δ 35.1 ppm.

Synthesis of Dianion 2. Two equivalents of methyllithium (4.0 mL, 1.6 M in diethyl ether, 6.4 mmol) was added to a solution of bis(diphenylthiophosphinoyl)methane (1.43 g, 3.2 mmol) in diethyl ether (20 mL) at −78 °C. The resulting mixture was warmed to room temperature and stirred for 3 h, leading to the formation of a yellow suspension of **2**. **2** was finally isolated as an etherate salt of the form **2B**·1.5Et_2O after evaporation of the solvents. Yield: 100% (1.71 g, 3.2 mmol). Selected data: ^{1}H NMR (300 MHz, C_6D_6, 25 °C) δ 0.71 ppm (t, $^{3}J_{HH} = 7.0$ Hz, 9H; Et_2O), 2.91 (t, $^{3}J_{HH} = 7.0$ Hz, 6H; Et_2O), 6.92 (m, 12H; H of phenyl groups (meta + para)), 7.92 (m, 8H; H of phenyl groups (ortho)); ^{31}P{^{1}H} NMR (121.5 MHz, C_6D_6, 25 °C, 85% H_3PO_4 as external standard) δ 23.4 ppm (s); ^{13}C{^{1}H} NMR (75.465 MHz, C_6D_6, 25 °C): δ 30.3 ppm (t, $^{1}J_{PC} = 41.1$ Hz; PCP), 128.0 (d, $^{3}J_{PC} = 11.5$ Hz; C_{meta}), 129.5 (bs, C_{para}), 132.4 (d, $^{2}J_{PC} = 11.2$ Hz; C_{ortho}), 143.9 (d, $^{1}J_{PC} = 73.2$ Hz; C_{ipso}). Anal. Calcd for $C_{62}H_{70}Li_4O_3P_4S_4$: C, 65.14; H, 6.17; Found: C, 65.18; H, 5.20. **2** might also be prepared in a toluene/ether mixture (5:1) by following the same procedure. In this case, **2** is characterized by a broad singlet at 24.3 ppm in ^{31}P NMR. The etherate complex **2A** was observed in the solid state and characterized only by X-ray diffraction analysis.

(65) Frisch, M. J.; Trucks, G. W.; Schlegel, H. B.; Scuseria, G. E.; Robb, M. A.; Cheeseman, J. R.; Montgomery, J. A., Jr.; Vreven, T.; Kudin, K. N.; Burant, J. C.; Millam, J. M.; Iyengar, S. S.; Tomasi, J.; Barone, V.; Mennucci, B.; Cossi, M.; Scalmani, G.; Rega, N.; Petersson, G. A.; Nakatsuji, H.; Hada, M.; Ehara, M.; Toyota, K.; Fukuda, R.; Hasegawa, J.; Ishida, M.; Nakajima, T.; Honda, Y.; Kitao, O.; Nakai, H.; Klene, M.; Li, X.; Knox, J. E.; Hratchian, H. P.; Cross, J. B.; Bakken, V.; Adamo, C.; Jaramillo, J.; Gomperts, R.; Stratmann, R. E.; Yazyev, O.; Austin, A. J.; Cammi, R.; Pomelli, C.; Ochterski, J. W.; Ayala, P. Y.; Morokuma, K.; Voth, G. A.; Salvador, P.; Dannenberg, J. J.; Zakrzewski, V. G.; Dapprich, S.; Daniels, A. D.; Strain, M. C.; Farkas, O.; Malick, D. K.; Rabuck, A. D.; Raghavachari, K.; Foresman, J. B.; Ortiz, J. V.; Cui, Q.; Baboul, A. G.; Clifford, S.; Cioslowski, J.; Stefanov, B. B.; Liu, G.; Liashenko, A.; Piskorz, P.; Komaromi, I.; Martin, R. L.; Fox, D. J.; Keith, T.; Al-Laham, M. A.; Peng, C. Y.; Nanayakkara, A.; Challacombe, M.; Gill, P. M. W.; Johnson, B.; Chen, W.; Wong, M. W.; Gonzalez, C.; Pople, J. A. *Gaussian 03*, revision C.02; Gaussian, Inc.: Wallingford, CT, 2004.

(66) Altomare, A.; Burla, M. C.; Camalli, M.; Cascarano, G.; Giacovazzo, C.; Guagliardi, A.; Moliterni, A. G. G.; Polidori, G.; Spagna, R. *SIR97*: An Integrated Package of Computer Programs for the Solution and Refinement of Crystal Structures using Single-Crystal Data.

(67) Sheldrick, G. M. *SHELXL-97*; Universität Göttingen, Göttingen, Germany, 1997.

(68) Grim, S. O.; Mitchell, J. D. *Inorg. Chem.* **1977**, *16*, 1762.

Synthesis of 4D. An excess of D_2O (0.10 mL, 5.5 mmol) was added to a suspension of dianion **6** (0.10 g, 0.28 mmol) in toluene (3 mL). The solvent was evaporated, and a CH_2Cl_2 (5 mL)/H_2O (5 mL) mixture was added. The organic layer was dried over Na_2SO_4. Pure **4D** was finally obtained after removal of the solvent in 94% yield (0.90 g, 0.26 mmol). Selected data: ^{1}H NMR (300 MHz, $CDCl_3$, 25 °C) δ 1.28 ppm (m, 24H; CH_3), 4.71 (m, 4H; CH); ^{31}P{^{1}H} NMR (121.5 MHz, C_6D_6, 25 °C, 85% H_3PO_4 as external standard) δ 17.9 ppm (s); ^{13}C{^{1}H} NMR (75.465 MHz, C_6D_6, 25 °C) δ 22.9 ppm (AXX′, $\sum J_{CP}$ = 17.4 Hz; CH_3), 23.1 (AXX′, $\sum J_{CP}$ = 16.4 Hz; CH_3), 26.2 (tq, $^1J_{CD}$ = 20.2 Hz, $^1J_{CP}$ = 137.3 Hz; PCP), 70.2 (AXX′, $\sum J_{CP}$ = 17.9 Hz; CH).

Synthesis of Dianion 6. Two equivalents of methyllithium (2.0 mL, 1.6 M in diethyl ether, 3.2 mmol) was added to a solution of tetraisopropylmethylenebisphosphonate (0.55 g, 1.6 mmol) and *N*,*N*,*N*′,*N*′-tetramethylethylenediamine (0.74 g, 6.4 mmol) in diethyl ether (10 mL) at low temperature (−78 °C). The resulting mixture was warmed to room temperature and stirred for 3 days, leading to the formation of a white precipitate of **6**. The sample was centrifuged, and the solvents were removed after decantation. Pure **6** was finally obtained as a white solid. Yield: 94% (0.53 g, 1.5 mmol). Anal. Calcd for $C_{13}H_{28}Li_2O_6P_2$: C, 43.84; H, 7.92; Found: C, 44.05; H, 7.98.

Synthesis of Dianion 7. One equivalent of carbon disulfide (0.15 g, 2.0 mmol) was added to a solution of dianion **2** (1.1 g, 2.0 mmol) in toluene (15 mL) at room temperature. The mixture was stirred for 12 h, leading to the formation of a yellow precipitate. This yellow solid was isolated after centrifugation and washed with a diethyl ether/hexanes mixture (1:1, 10 mL). Pure dianion **7** was finally isolated as a yellow solid in 95% yield (1.44 g, 1.9 mmol). Selected data: ^{1}H NMR (300 MHz, d_5-pyridine, 25 °C) δ 7.04 ppm (m, 12H; H of phenyl groups (meta + para)), 8.53 (m, 8H; H of phenyl groups (ortho)); ^{31}P{^{1}H} NMR (121.5 MHz, d_5-pyridine, 25 °C, 85% H_3PO_4 as external standard) δ 38.0 ppm (s); ^{13}C{^{1}H} NMR (75.465 MHz, d_5-pyridine, 25 °C) δ 87.8 ppm (t, $^1J_{PC}$ = 93.5 Hz; PCP), 127.0 (vt, $\sum J_{PC}$ = 11.8 Hz, C_{meta} of phenyl groups), 128.1 (bs; C_{para} of phenyl groups), 132.0 (bs; C_{ortho} of phenyl groups), 139.5 (bs; C_{ipso} of phenyl groups), 225.3 (t, $^2J_{PC}$ = 5.2 Hz; SCS). Anal. Calcd for $C_{38}H_{50}Li_2O_3P_2S_2$: C, 60.14; H, 6.64; Found: C, 60.19; H, 6.71.

Synthesis of Dianion 8. A large excess of carbon disulfide (0.38 g, 5.0 mmol) was added to a solution of dianion **6** (0.18 g, 0.50 mmol) in toluene (10 mL) at room temperature. The mixture was stirred at room temperature, and the solution turned yellow over a period of 10 days. Evaporation of the solvent and excess CS_2 afforded a yellow solid, which was washed with a toluene/hexanes mixture (1:3, 10 mL). Pure **8** was finally isolated as a yellow solid in 87% yield (0.19 g, 0.43 mmol). Selected data: ^{1}H NMR (300 MHz, C_6D_6, 25 °C) δ 4.71 ppm (bs, 4H; ^{i}Pr), 1.36 (bs, 12H; ^{i}Pr); ^{31}P{^{1}H} NMR (121.5 MHz, C_6D_6, 25 °C, 85% H_3PO_4 as external standard) δ 25.3 ppm (bs); ^{13}C{^{1}H} NMR (75.465 MHz, d_8-THF, 25 °C) δ 24.9 ppm (bs; ^{i}Pr), 70.1 (bs; ^{i}Pr), PCP not observed, 227.4 (bs; SCS). Anal. Calcd for $C_{14}H_{28}Li_2O_6P_2S_2$: C, 38.89; H, 6.53; Found: C, 39.16; H, 6.54.

Synthesis of 9. Two equivalents of butyl iodide (0.37 g, 2.0 mmol) was added to a solution of **7** (0.76 g, 1.0 mmol) in THF (15 mL). The solution was stirred for 12 h at room temperature. Pure **9** was finally isolated as a yellow solid after evaporation of the solvent. Yield: 100% (0.63 g, 1.0 mmol). Selected data: ^{1}H NMR (300 MHz, d_8-THF, 25 °C) δ 0.66 ppm (t, $^3J_{HH}$ = 7.2 Hz, 6H, butyl), 0.76 (m, 4H; butyl), 0.98 (m, 4H; butyl), 2.33 (m, 4H; butyl), 6.94−7.96 (m, 20H; H of phenyl groups); ^{31}P{^{1}H} NMR (121.5 MHz, d_8-THF, 25 °C, 85% H_3PO_4 as external standard) δ 41.4 ppm (s); ^{13}C{^{1}H} NMR (75.465 MHz, d_8-THF, 25 °C) δ 13.6 ppm (s; butyl), 22.7 (s; butyl), 30.3 (s; butyl), 36.4 (s; butyl), 125.7 (t, $^1J_{PC}$ = 64.5 Hz; PCP), 128.2−132.3 (m; C of phenyl groups), 175.9 (t, $^2J_{PC}$ = 2.7 Hz, SCS). Anal. Calcd for $C_{34}H_{38}P_2S_4$: C, 64.12; H, 6.01; Found: C, 64.15; H, 6.09.

Synthesis of 10. An excess of butyl iodide (0.55 g, 3.0 mmol) was added to a solution of **8** (0.13 g, 0.3 mmol) in toluene (5 mL), and the mixture was stirred for 2 days at room temperature. Evaporation of the solvent and remaining butyl iodide affords a yellow solid of pure **10**. Yield: 100% (0.16 g, 0.3 mmol). Selected data: ^{1}H NMR (300 MHz, CD_2Cl_2, 25 °C) δ 0.93 ppm (t, $^3J_{HH}$ = 7.5 Hz, 6H; butyl), 1.31 (d, $^3J_{HH}$ = 6.1 Hz, 12H, ^{i}Pr), 1.38 (d, $^3J_{HH}$ = 6.1 Hz, 12H, ^{i}Pr), 1.42 (m, 4H; butyl), 1.65 (m, 4H; butyl), 3.03 (t, $^3J_{HH}$ = 7.5 Hz, 4H; butyl), 5.0 (m, 4H; ^{i}Pr); ^{31}P{^{1}H} NMR (121.5 MHz, CD_2Cl_2, 25 °C, 85% H_3PO_4 as external standard) δ 11.5 ppm (s); ^{13}C{^{1}H} NMR (75.465 MHz, CD_2Cl_2, 25 °C) δ 13.6 ppm (s; butyl), 22.3 (s; butyl), 24.0 (t, $^3J_{PC}$ = 2.4 Hz; ^{i}Pr), 24.1 (t, $^3J_{PC}$ = 2.3 Hz; ^{i}Pr), 31.9 (s; butyl), 38.1 (s; butyl), 74.0 (bs; ^{i}Pr), PCP not observed, 183.7 (bs; SCS). Anal. Calcd for $C_{22}H_{46}O_6P_2S_2$: C, 49.61; H, 8.70; Found: C, 49.84; H, 8.70.

Acknowledgment. We thank the CNRS (Centre National de la Recherche Scientifique) and the Ecole Polytechnique for the financial support of this work and IDRIS (Orsay, Paris XI, project No. 51616) for the allowance of computer time.

Supporting Information Available: NBO analysis of hyperconjugative interactions in **B**−**D** (Tables S1 and S2), tables, figures, and CIF files giving crystallographic data for **2A**, **2B**, **7**, and **9**, and tables and figures giving optimized geometries and frequencies for compounds **A**−**J** and **TSG**−**TSJ**. This material is available free of charge via the Internet at http://pubs.acs.org.

OM060450L